

across the 8 measurement positions, is small and similar for both systems (both <0.25). In the y-direction the mean gamma index is similar for both systems and decreases with increasing energy, but is always less than 0.5.

Conclusions: Both systems produce beam models within clinically-accepted tolerances however the differences in algorithms lead to minor fitting differences. Perhaps the most important difference is Pinnacle's consistent overestimation of the Bragg peak depth (0.3mm on average). It should be noted however that this problem has since been addressed in the latest Pinnacle update (July 2012), to allow an increased weighting to be placed on the distal edge during the fitting process. It would be of interest to investigate how the fitting errors translate to benchmarking in a phantom.

PD-0571

Is the TPS photon field implementation detector-depending?

M. Fortunato¹, P. Colleoni¹, S. Andreoli¹, M. Di Martino¹, R. Moretti¹
¹Ospedali Riuniti di Bergamo, USC Fisica Sanitaria, Bergamo, Italy

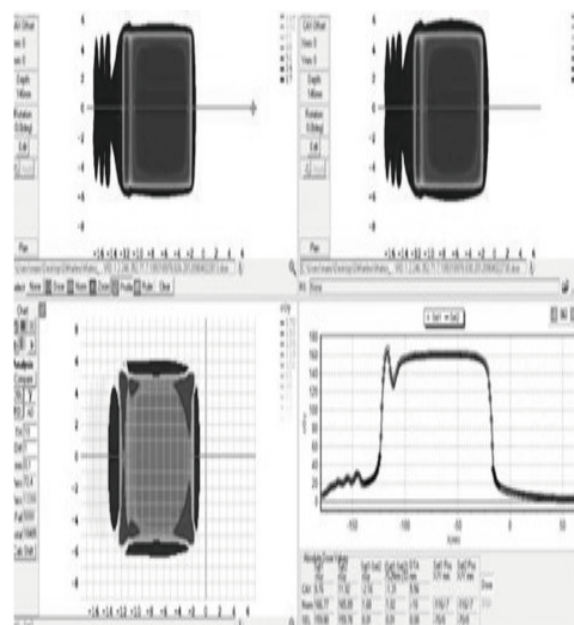
Purpose/Objective: The dosimetric characterization of a photon field can show relevant differences depending on the used detectors. The focus of this work is to evaluate the influence of these differences in Treatment Planning System (TPS) algorithm, implementing different machines (each one for every detector, i.e. 'detector-machine'). Validated the reliability of the algorithm for our reference detector-machine by the IAEA TECDOC 1540 and 1583, the comparison among the detector-machines could be made for different plans in water, slab antropomorphic phantom and on clinical CT images by the $\Gamma(\delta x, \delta d)$ function.

Materials and Methods: A 6MV photon field (Varian Clinac 6EX) was implemented with Varian Eclipse AAA algorithm (v.10.0.28). The Dose Profiles, the Percentual Depth Dose and the Output Factors (open fields, 2x2 to 40x40 cm) have been measured for each detector-machine. The different machines were obtained with the following PTW detectors: μ Lion, semiflex 0.125, unshielded diode and diamond. The μ Lion-machine has been chosen as reference after being validated with IAEA TECDOC 1540 and 1583 tests in water and in slab phantom (Easy-Cube, Euromechanics) by a semiflex 0.125 chamber for dose point calculation. Then the $\Gamma(\delta x, \delta d)$ function was evaluated matching fourteen plan dose matrices extracted from the TPS for different plans studied with each detector-machine in water, in the slab phantom and by plans based on clinical TC images for the breast, lung and pelvis districts. Two dose deviation/error position criteria have been considered: 3%/1mm (TPS calculation grid) and 1%/0,1mm. Because the dose matrices were calculated on the same TC images, the positional error Δx in $\Gamma(\delta x, \delta d)$ function can be considered null, so $\Gamma(\delta x, \delta d) = \Gamma(\delta d)$.

Results: The IAEA validation tests shown that the μ Lion-machine was in good agreement with the dose tolerance recommended value. Among the fourteen plan dose matrices, in table are presented the worst case comparison between machines (respect to μ Lion-machine).

Detector	Criteria	
	3% , 1mm	1% , 0.1mm
semiflex 0.125	0.2 %	6.0 %
unshielded diode	1.7 %	27.6 %
diamond	34.2 %	74.7 %

Conclusions: In relative field characterization, substantial differences were observed at the edges profiles and for points at pre-buildup and over 30 cm depths. The 3%/1mm criteria shows no significant differences, while the second one emphasizes coincidences between the two ion chambers (semiflex and μ Lion). There are evidence of differences in calculated dose in anatomical regions with high gradient density (see the attached figure where the comparison between μ Lion and unshielded diode detector-machine for a 10x10cm field is shown), but negligible considering the criteria of comparison. Experimental verification with detector arrays (MapCheck and ArcCheck SNC) are in progress.



POSTER DISCUSSION: YOUNG SCIENTISTS 7: IMAGE REGISTRATION AND MANAGEMENT OF INTRA- AND INTERFRACTION MOTION

PD-0572

Physical validation of a deformable CT-CBCT registration tool for IGRT

L. Boldrini¹, L. Placidi², G.C. Mattiucci¹, G.R. D'Agostino¹, D. Raspanti³, V. Valentini¹, A. Fidanzio²

¹Università Cattolica del Sacro Cuore, Radiation Oncology, Rome, Italy

²Università Cattolica del Sacro Cuore, Medical Physics, Rome, Italy

³Tema Sinergie, Faenza, Italy

Purpose/Objective: Deformable registrations between simulation CT and CBCT images were performed by the MIM 5.5.2 software in order to assess its capability in accounting for organ movement and morphologic variations.

Materials and Methods: Two phantoms were realized with different density inserts and a fixed structure (to simulate bone structures). Two different configurations for each phantom were designed: the first one was acquired only by CT scanner, the second one, with modified dimensions and positions of the insert, was acquired by CT scanner and three CBCT image acquisition protocols (high, medium and low definition: HD, MD, LD). In the second phantom configuration, the volumes of the insert were reduced between 20% and 60% and its geometric positions were changed within 1 cm. All the structures were contoured. Deformable registrations were performed by MIM 5.5.2 software, obtaining surrogate images with autocontoured inserts. In particular for each phantom the first configuration CT images were deformed on the CT and CBCT images of the second configuration. Volume differences, HU differences, centroid's coordinates difference, Pearson coefficients and Dice Similarity Index (DSI) were determined between the surrogates and the images of the second configuration phantoms, to assess the fusion algorithm.

Results: For the surrogates obtained by the registration of the CT images of the two phantom configurations, Pearson correlation coefficient equal to 0.996, insert volume variations within 2%, mean insert HU variations within 1.5%, centroid's coordinate variations within 1mm and DSI values equal to 0.99, were observed. Regarding the surrogate obtained by the deformable registration of the CT with the different CBCT resolutions (high, medium and low), we observed Pearson coefficient correlation variation from 0.997 to 0.995, insert volume variations range between 6% and 8%, mean insert HU range from 5% to 9%. The centroid's coordinate variations are within 1mm and the Dice values changes between 0.91-0.97. (Tab.1)

	CT	CBCT HD	CBCT MD	CBCT LD
Pearson coefficient	0.996	0.997	0.997	0.995
Volume variation	2%	6.9%	7.6%	8.1%
Mean HD variation	1.5%	5.5%	6.0%	8.8%
Centroid variation (mm)	<1	<1	<1	<1
DSI range	0.98-0.99	0.93-0.97	0.91-0.95	0.94-0.96

Conclusions: The deformable registration obtained by MIM 5.5.2 software is reliable, especially considering that the insert movements and morphologic variations were intentionally macroscopic. Further studies are however required to assess its applicability in everyday clinical IGRT practice.

PD-0573

Assessment of accuracy of non-rigid registration algorithms for follow-up treatment NSCLC imaging

J.M. Spijkerman¹, D. Fontanarosa², W. van Elmpt¹

¹MAASTRO GROW Research Institute, Department of Radiation Oncology, Maastricht, The Netherlands

²Philips Research, Minimally Invasive Healthcare, Eindhoven, The Netherlands

Purpose/Objective: In lung cancer patients, accurate registration of follow-up imaging to pre-treatment information is hampered by possible large deformations induced by the (chemo-) radiotherapy treatment. To register on a tumour level and subsequently on a sub-volume level inside the tumour, non-rigid registration algorithms might be applied. A validation study was performed on the accuracy of two commonly used deformation models for the registration of pre- and post-treatment PET/CT scans of lung cancer patients undergoing radiotherapy.

Materials and Methods: For 3 patients, we annotated both a pre-treatment and 3 months post-treatment CT scan using approximately 30 visible landmarks/fiducials per patient. This included approx. 10 landmarks inside or directly surrounding the primary tumour. These landmarks were selected based on visible features inside the thorax, e.g. bifurcating vessels, calcifications, distinct anatomical shapes. Rigid registration served as the starting point. Non-rigid registration was performed using either a Demons or Morphons algorithm, with 10 or 20 iterations per scale (10 resolution scales used), using a weighted sum accumulation or a diffeomorphic accumulation of the deformation field; leading to 8 different deformation fields. Absolute differences in deformed and annotated landmark position were calculated and compared between these algorithms.

Results: Differences in landmark positions (mean±1SD) for the three patients decreased from 6±2, 9±4 and 9±4 mm for the rigid registration to a best [worst] result for the 8 different algorithms between: 3±2 [4±3], 3±2 [6±3] and 6±4 [7±5] mm, respectively. For the landmarks close to the tumour a similar result was achieved: rigid 6±2, 10±4 and 10±4 mm reduced to 3±2, 2±2 and 9±5 mm for the best performing non-rigid registration method. The Morphons registration with diffeomorphic accumulation and 20 iterations per scale outperformed the other methods in 5 out of 6 of the above mentioned cases.

Conclusions: Non-rigid registration techniques are accurate within (on average) 3-6 mm for registration of pre-treatment and follow-up imaging. As expected, there is a large improvement over rigid registration where differences can be up to 1 cm. The deformation methods need to be further optimized but may play a role in the analysis of follow-up imaging for assessment of local control and recurrences of sub-volumes of the primary tumour.

PD-0574

Deformable multimodal image registration strategies for the integration of PET/MR data into radiotherapy planning

S. Leibfarth¹, D. Mönlich¹, S. Welz², N. Schwenzer³, H. Schmidt³, D. Zips², D. Thorwarth¹

¹University Hospital Tübingen, Section for Biomedical Physics, Tübingen, Germany

²University Hospital Tübingen, Department of Radiation Oncology, Tübingen, Germany

³University Hospital Tübingen, Department of Diagnostic and Interventional Radiology, Tübingen, Germany

Purpose/Objective: The integration of PET/MR information into radiotherapy (RT) seems to be highly beneficial due to the additional molecular, functional and anatomical information. Thus, the purpose

of this study was to develop a suitable registration strategy for the fusion of PET/MR and CT in the head and neck (HN) region.

Materials and Methods: Seven HN patient datasets with corresponding clinical PET/CT and directly following PET/MR were available, with FDG as PET tracer. For the registration, only CT and MR were considered. After a rigid registration, a deformable registration with a transformation parametrized by B-splines was performed, with three different strategies for the metric to be optimized: global mutual information (MI) (GMI), GMI combined with a bending energy penalty (BEP) term (GMI+BEP) and localized MI combined with BEP (LMI+BEP). For each strategy, optimal values for registration parameters were determined on the basis of quantitative registration quality measures. As anatomic quality measures the Dice Similarity Index (DSI) of skin, common carotid arteries and respiratory tract as well as the non-overlapping fraction (NOF) of the spinal canal as derived from the MR with vertebral bodies segmented on the CT were used. As a functional measure the Normalized Cross Correlation (NCC) of the PET images in a region containing the GTV was introduced. Each measure yields values between 0 and 1, with 1 being the best result. Furthermore, anatomical landmarks were defined by an experienced radiation oncologist for which the mean distance after registration was determined. Additionally, the fused images as well as the Jacobian determinants of the resulting displacement fields were visually inspected.

Results: For each registration strategy, the obtained quality measures are shown in Table 1 as the mean of all seven patients. Using GMI only, some of the measures became worse compared to rigid registration. However, for GMI+BEP and LMI+BEP all measures improved, indicating a good registration accuracy. In particular, the functional measure defined on a voxel basis in a low-contrast region improved simultaneously with the anatomically defined measures. Overall, LMI+BEP yields the best and most robust results. Visual inspection of the Jacobian determinant favors GMI+BEP and LMI+BEP, whereas GMI suffers from unrealistically high, low, and even partially negative values.

Table 1: Registration quality measures for different registration strategies.

	rigid	GMI	GMI+BEP	LMI+BEP
DSI skin	0.90	0.92	0.92	0.93
DSI carotids	0.29	0.18	0.56	0.64
DSI respiratory tract	0.44	0.50	0.65	0.71
NOF bone/spinal canal	0.56	0.72	0.75	0.92
NCC PET	0.73	0.50	0.83	0.86
landmark distances (mm)	5.50	8.95	3.70	3.10

Conclusions: For the deformable registration of PET/MR and PET/CT in the HN region, a suitable registration strategy could be determined. For a B-spline parametrized registration in combination with MI, a regularization consisting of a BEP significantly improves registration results and robustness. Also the localized form of MI is favorable. As a consequence, B-spline registration strategies including BEP should be used for the integration of functional PET/MR data into individualized RT planning.

PD-0575

How accurate a segmentation could be? Evaluation of consistence and coherence of an elastic deformation algorithm

L. Schiappacasse¹, R. Viard², D. Gibon², T. Laceronerie¹, T. Leroy¹, G. Lodron³, F. Vasseur¹, E. Lartigau¹

¹Centre Oscar Lambret, Département Universitaire de Radiothérapie, Lille, France

²AQUILAB SAS, Recherche & Développement Avancé, Lille, France

³Joanneum Research, Machine Vision Applications, Graz, Austria

Purpose/Objective: The Adaptive Radiotherapy approach has been supported by an increasing amount of clinical data that has shown the impact of anatomical modifications during Radiotherapy. This technique is not used in clinical routine because the additional treatment planning required to take account of the anatomical modifications is considered too expensive in time, especially because of the need of new 'adapted contours'.

The automated adaptation of RT-structures should alleviate this problem, but clinical validation of deformable image registration tools is needed.